

# Cracking the Microsecond: An Efficient and Precise Time Synchronization Scheme for Hybrid 5G-TSN Networks

Michael Gundall\* and Hans D. Schotten\*‡

\*German Research Center for Artificial Intelligence (DFKI), Kaiserslautern, Germany

‡Department of Electrical and Computer Engineering, RPTU University Kaiserslautern-Landau, Kaiserslautern, Germany

Email: {michael.gundall, hans\_dieter.schotten}@dfki.de

**Abstract**—Achieving precise time synchronization in wireless systems is essential for both industrial applications and 5G, where sub-microsecond accuracy is required. However, since the Industrial Internet of Things (IIoT) market is negligible compared to the consumer electronics market, the so-called IIoT enhancements have not yet been implemented in silicon. Moreover, there is no guarantee that this situation will change soon. Thus, alternative solutions must be explored.

This paper addresses this challenge by introducing a scheme that uses a protocol capable of leveraging existing infrastructure to synchronize User Equipments (UEs), with one of the UEs serving as the master. If this master is connected via a wired link to the factory network, it can also function as a boundary clock for the factory network, including any Time-Sensitive Networking (TSN) network. Furthermore, the 5G Core Network (5GC) and 5G Base Station (gNB) can also be synchronized if they are connected either to the factory network or to the master UE.

The proposed solution is implemented and evaluated on a hardware testbed using OpenAirInterface (OAI) and Software Defined Radios (SDRs). Time offset and clock skew are analyzed using a moving average filter with various window sizes. Results show that a filter size of 1024 provides the best accuracy for offset prediction between UEs. In a controlled lab environment, the approach consistently achieves synchronization within  $\pm 50$  ns, leaving sufficient margin for synchronization errors in real deployments while still maintaining sub-microsecond accuracy. These findings demonstrate the feasibility and high performance of the proposed protocol for stringent industrial use cases.

**Index Terms**—Wireless Time Synchronization, 5G, TSN, Testbed

## I. INTRODUCTION

Precise time synchronization is a fundamental requirement of modern information and communication technology (ICT) systems on earth and beyond [1]. This is especially true for industrial applications, where stringent Real-Time (RT) performance is crucial. In particular, synchronicity of less than 1  $\mu$ s is

This research was supported by the German Federal Ministry of Research, Technology and Space (BMFTR) within the projects Open6GHub and 6GTerfactory under grant numbers 16KISK003K and 16KISK186. The responsibility for this publication lies with the authors. This is a preprint of a work accepted but not yet published at the 2025 IEEE International Symposium on Precision Clock Synchronization for Measurement, Control, and Communication (ISPCS). Please cite as: M. Gundall and H. D. Schotten: “Cracking the Microsecond: An Efficient and Precise Time Synchronization Scheme for Hybrid 5G-TSN Networks”. In: 2025 IEEE International Symposium on Precision Clock Synchronization for Measurement, Control, and Communication (ISPCS), IEEE, 2025.

mandated for demanding RT class C use cases, ensuring deterministic behavior in automated industrial environments [2]. For emerging 5G-Advanced and 6G use cases, the requirement of one microsecond remains relevant [3]. Additionally, precise synchronization is necessary to avoid interference in Time Division Duplex (TDD) systems, which are increasingly used, for example, in frequency band n78, which serves for private networks in Germany, and in FR2 (mmWave) bands.

While wireline solutions, such as the White Rabbit extension of the Precision Time Protocol (PTP), can achieve synchronization accuracies down to 100 ps [4], extending this level of precision to wireless systems remains challenging. The inherent characteristics of wireless communication, such as mobility, varying channel conditions, packet loss and line-of-sight constraints, present challenges in meeting the requirements [5].

In response to these challenges, 5G Release 16 and 17 specifications introduce concepts aimed at fulfilling the synchronization requirements for Industrial Internet of Things (IIoT). However, practical implementation by chipset manufacturers is unlikely, as the IIoT market segment often lacks the scale and profit margins necessary to justify the investment, especially compared to the consumer market. Consequently, alternative methods must be explored to meet stringent timing demands of mobile use cases.

One potential approach is the tunneling of PTP messages within 5G data packets [6]. Nevertheless, this method typically relies on software timestamps, in order to use existing hardware. Consequently, only millisecond-level accuracy is reached using this approach, falling short of industrial synchronization requirements [6]. Another promising alternative leverages the broadcast nature of wireless systems, which, while often considered a drawback due to interference and lack of determinism, can be exploited effectively for one-way time synchronization protocols. In this context, the so-called Reference Broadcast Infrastructure Synchronization (RBIS) protocol is a viable solution [7]. Originally developed for Wi-Fi networks, RBIS is adaptable to any infrastructure-based wireless communication system, including 5G. Moreover, RBIS requires no modifications to existing network infrastructure, allowing seamless integration with standard 5G Base Stations (gNBs).

Additionally, RBIS supports the inclusion of external time sources, facilitating the realization of hybrid networks that

converge 5G and Time-Sensitive Networking (TSN), as found in modern smart factories. Owing to these strengths, RBIS serves as the foundation for the investigations presented in this paper, which aims to evaluate its feasibility and performance in meeting the stringent synchronization requirements of industrial 5G use cases.

Accordingly, the following contributions can be found in this paper:

- Scheme for efficient and precise time synchronization in hybrid 5G-TSN networks.
- Evaluation on a testbed demonstrating sub-microsecond accuracy and precision.

Accordingly, the rest of the paper is structured as follows: Section II introduces related work. Furthermore, the proposed Scheme for achieving highly synchronized 5G-TSN networks is presented in Section III. Then, the experimental setup is introduced in Section V. Thereafter, the used methodology is explained in Section IV and the results are discussed in Section VI. Finally, Section VII concludes the paper.

## II. RELATED WORK

Time synchronization in cellular systems gained attention with Industry 4.0 use cases requiring sub-microsecond accuracy for high-performance wireless communications [8], [9]. 3GPP Release 16 introduced 5G synchronization targets of  $1\text{ }\mu\text{s}$  [10]. Both Device-Side TSN Translator (DS-TT) and Network-Side TSN Translator (NW-TT) have been proposed to integrate 5G in factory networks [11].

Research on applying PTP in 5G revealed millisecond-level precision limitations due to tunneling in the data plane [6]. Other studies reported synchronization accuracy between User Equipment (UE) and gNB in the  $470 - 540\text{ ns}$  range [12], though lacking testbed evaluations. The authors in [13] implemented a TSN translator hardware testbed achieving  $1 - 10\text{ }\mu\text{s}$  accuracy. Propagation delay compensation as well as elimination of other error sources remains challenging, as discussed in [14].

Most industrial devices are serving as UEs, making synchronization between them more important than of a UE with the gNB from an application point of view. Thus, the RBIS protocol, originally proposed for Wi-Fi, is well suited for this purpose [7]. Prior work achieved sub-millisecond requirements [15] and  $\pm 10\text{ }\mu\text{s}$  accuracy with offset correction in distributed setups [16]. To our knowledge, consistent microsecond-level synchronization has not yet been demonstrated. Our work attempts to improve on this by applying both offset and rate correction, leveraging precise hardware timestamps from Software Defined Radio (SDR) clocks, which are more stable than CPU clocks that were used before.

## III. EFFICIENT AND PRECISE TIME SYNCHRONIZATION SCHEME FOR HYBRID 5G-TSN NETWORKS

This section introduces the concept that enables efficient and precise time synchronization in hybrid 5G-TSN networks. First, the RBIS protocol, which serves as the basis for this approach, is presented in Section III-A. Although it has certain prerequisites, it is technology independent and its mapping to 5G systems

is described in Section III-B. Furthermore, protocol extensions that make it well suited for hybrid 5G-TSN networks as well as the architectural integration possibilities are proposed in Section III-C.

### A. RBIS Protocol

Figure 1 depicts the Message Sequence Chart (MSC) of the protocol. Upon reception of a SYNC signal transmitted by the

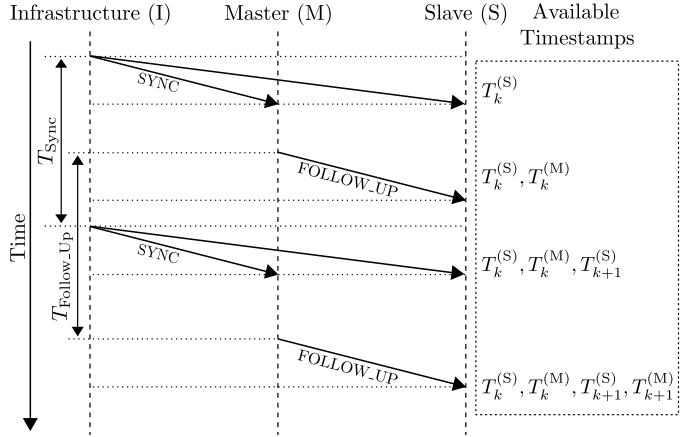


Figure 1. MSC of technology-independent RBIS protocol.

infrastructure, each device generates a timestamp based on its individual clock. Subsequently, the master transmits its “correct” timestamps, denoted by  $T_k^{(M)}$ , to all slaves via the FOLLOW\_UP message. Subsequently, each slave generates its own reference timestamps, denoted by  $T_k^{(S)}$ . The resulting  $T_k^{(M)}$  and  $T_k^{(S)}$  tuples are used to estimate the offset  $\theta$  and skew  $\gamma$  between the master and slave clocks following Equations 1-2 [17].

$$\hat{\theta}_K = T_k^{(S)} - T_k^{(M)} \quad (1)$$

$$\hat{\gamma}_k = \frac{\hat{\theta}_k - \hat{\theta}_{k-1}}{T_k^{(M)} - T_{k-1}^{(M)}} \quad (2)$$

Additionally, the repetition intervals of both SYNC and FOLLOW\_UP messages do not have to be the same.

### B. Mapping to 5G

In order to make the RBIS protocol applicable to 5G, a potential synchronization signal has to be identified that serves as SYNC message and must contain a unique identifier that allows to differ upcoming from preceding signals. Here, the so-called Physical Broadcast Channel (PBCH), which is co-located to Primary Synchronization Signal (PSS) and Secondary Synchronization Signal (SSS), and can be found inside the Synchronization Signal Block (SSB), is well suited. Moreover, the PBCH carries the so-called System Frame Number (SFN). The SFN is of interest because it is a cyclically incremented identifier. Furthermore, it is incremented every 1 ms and has a length of 10 bit. So the maximum value is 1023 and a repetition occurs every 10.24 s. This means that the second criterion for assigning a timestamp to an unique message can only be

partially fulfilled, however, an initial offset of  $\theta_0 < 10.24/2$  s = 5.12 s can easily be guaranteed by sending an initial timestamp  $\theta_0$ . Moreover, the PBCH is sent in an interval between 5 ms and 160 ms and can serve as  $T_{Sync}$  variable of the RBIS protocol.

### C. Protocol Extensions and Architectural Integration

This section introduces the existing 5G-specific protocol extensions and suggests how the RBIS protocol can be integrated into hybrid networks. As illustrated in Figure 2, the

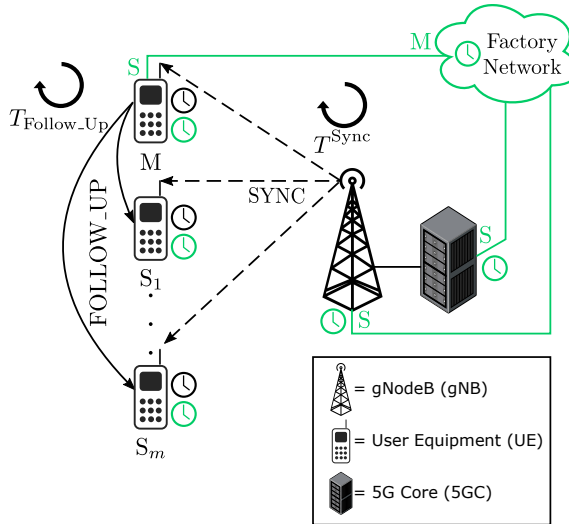


Figure 2. Architectural integration possibilities of the RBIS protocol in hybrid 5G-TSN networks.

RBIS protocol does not compensate the signal propagation time, which is negligible in Wi-Fi deployments, due to the typically small spatial coverage. However, in 5G scenarios where larger spatial coverage is feasible, variations in the distance between the UEs and the gNB can introduce runtime errors in the synchronization. To mitigate this, the so-called Timing Advance (TA), which is calculated by the gNB and transmitted to the UEs, can be utilized to compensate for propagation-induced delays and improve synchronization accuracy [9].

Furthermore, in its current form, the protocol synchronizes only the UEs within a single cell. To extend synchronization coverage beyond a single cell, concepts for expanding the coverage area both non-invasively and invasively have been proposed, with the latter approach aligning with the evolution towards future 6G networks [18].

In order to synchronize the UEs to a TSN master clock, the master UE can be connected wireline to the factory network. Hence, a single UE needs to be stationary, but can serve as boundary clock between UEs and TSN components. Consequently, the time of a TSN master located in the factory network can also be distributed to all UEs. Thus, the remaining limitation of the protocol, namely its inability to synchronize UEs with gNB and 5G Core Network (5GC), is lifted.

## IV. EXPERIMENTAL SETUP

The experimental setup is shown in Figure 3. It consists of general-purpose computing hardware, SDRs, and measurement

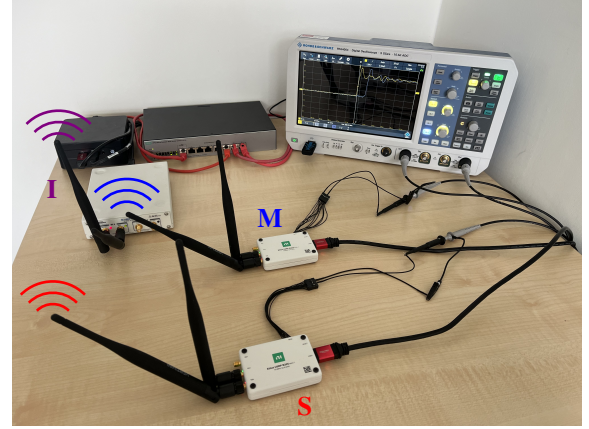


Figure 3. Experimental setup consisting of a mini PC, one USRP B210 as gNB, two USRP B205mini as UEs, and an oscilloscope.

Table I  
HARDWARE CONFIGURATIONS

Equipment	QTY	Specification
Mini PC	1	13 <sup>th</sup> Gen. Intel Core i7-1360P, 32 GB DDR4, 3x USB 3.2 Gen2 Ubuntu 24.04.2 LTS 64-bit
5G gNB	1	Ettus Research USRP B210
5G UE	2	Ettus Research USRP B205mini
Oscilloscope	1	Rohde&Schwarz RTA4004

equipment, as summarized in Table I. The core processing unit is a mini PC equipped with an Intel Core i7 CPU and 32 GB of DDR4 RAM. The system runs Ubuntu 24.04.2 LTS (64-bit). The entire 5G system is implemented using the OpenAirInterface (OAI)<sup>1</sup> open-source software suite. Specifically, the 5GC, gNB, and UE functionalities are all executed concurrently on the same mini PC, enabling an integrated and reproducible 5G setup. This is possible, as the selected mini PC has three high speed USB ports.

For the radio access network, an Ettus Research USRP B210 SDR is used as gNB, denoted by I. It supports RF frequencies from 70 MHz to 6 GHz with a 2x2 MIMO configuration and a Spartan 6 FPGA. Hence, they are suitable to operate in frequency band n78 that is used for private networks in Germany. Moreover, two Ettus Research USRP B205mini SDRs serve as UEs (M and S), which provide similar RF capabilities and, importantly, feature accessible GPIO pins. One GPIO pin from each B205mini device is connected to a channel of a Rohde & Schwarz RTA4004 oscilloscope, which operates with a maximum sampling rate of 5 GSa/s. This enables high-resolution measurement of the generated validation signals, allowing precise offset measurements to evaluate the time synchronization error between both UEs.

<sup>1</sup><https://gitlab.eurecom.fr/oai/openairinterface5g/>

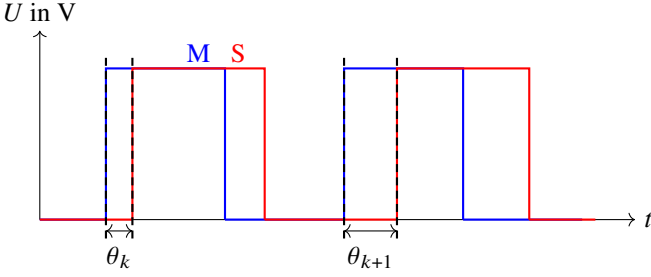


Figure 4. Offset between two rectangular signals over time.

## V. METHODOLOGY

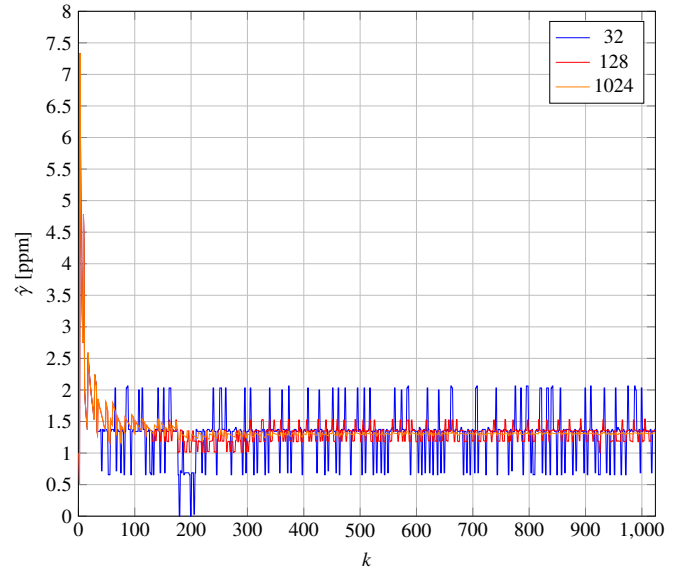
To evaluate the clock synchronization performance between two UEs, a measurement procedure is implemented to estimate clock skew and clock offset over time. To mitigate short-term noise and measurement fluctuations, a moving average filter of size  $N$  is applied to estimate the underlying clock skew. Using this prediction, the offset at a future time instant can then be determined by integrating the estimated drift over time and adding it to the last measured offset. To evaluate the achievable accuracy and precision, each UE periodically generates a rectangular signal via its accessible GPIO pin. As shown in Figure 4, two such signals, one from each UE, are generated with voltage levels varying between 0 V (logical 0) and 3.3 V (logical 1). These signals are generated on the USRPs using timed commands to ensure deterministic signal generation aligned with their hardware clock. Both signals are captured simultaneously using the oscilloscope. By comparing the time stamps of rising or falling edges of the two validation signals, the instantaneous clock offset between the UEs can be determined. Repeated measurements over an extended period allow observation of how this offset evolves over time due to clock skew.

## VI. EVALUATION

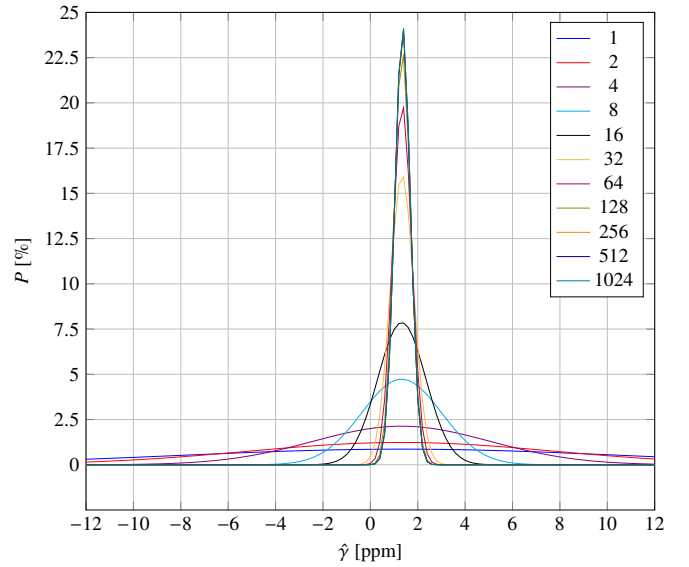
In this section, the proposed time synchronization scheme is evaluated in detail. First, the clock skew is identified in Section VI-A, and based on these measurements, an appropriate filter size is selected and integrated into the algorithm. This is followed by the presentation of offset measurement results in Section VI-B, which demonstrate precision and accuracy of the synchronization scheme.

### A. Identification of Clock Skew

A measurement series consisting of 1,000 samples was conducted using the described methodology to ensure statistical reliability. Figure 5 illustrates the convergence of the skew estimation for three different filter sizes, denoted by  $N$ , (see Figure 5a) as well as the statistical distribution of all tested values (see Figure 5b). It is visible, that the filter for  $N = 1024$  converges at 1.36 ppm, while skew estimation of  $N = 32$  jumps between 0.75 ppm and 2 ppm. The detailed statistical characteristics of the estimated clock skew  $\hat{\gamma}$  for various moving



(a) Time series obtained for the readings of estimated clock skew  $\hat{\gamma}$ .



(b) Distribution functions obtained for the readings of estimated clock skew  $\hat{\gamma}$ .

Figure 5. Illustration of the convergence behavior of the clock skew estimation with increasing filter size  $N$  of the moving average filter and corresponding statistical distributions.

average filter sizes are summarized in Table II. The table reports the median  $\tilde{x}$ , mean  $\bar{x}$ , standard deviation  $\sigma$ , and the intervals  $2\sigma$  and  $3\sigma$ , with all values rounded to four decimal places. As observed, increasing the filter size  $N$  significantly reduces the standard deviation  $\sigma$ , indicating that the moving average filter effectively suppresses high-frequency noise and fluctuations in the clock skew estimate. Specifically,  $\sigma$  decreases from 9.2491 ppm for  $N = 1$  to 0.3282 ppm for  $N = 1024$ . Correspondingly, the uncertainty intervals  $2\sigma$  and  $3\sigma$  shrink proportionally, demonstrating a substantial improvement in estimation precision.

The mean shows a slight increasing trend with larger  $N$ ,

Table II

STATISTICAL MEASUREMENTS MOVING AVERAGE FILTER OF SIZE  $N$   
FOR ESTIMATED CLOCK SKEW  $\hat{\gamma}$ .

$N$	$\tilde{x}$	$\bar{x}$	$\sigma$	$2\sigma$	$3\sigma$
<b>1</b>	0.0000	1.3145	9.2491	18.4982	27.7472
<b>2</b>	0.0000	1.3149	6.4737	12.9473	19.4210
<b>4</b>	0.0000	1.3167	3.7437	7.4875	11.2312
<b>8</b>	0.0000	1.3201	1.6869	3.3738	5.0607
<b>16</b>	1.3750	1.3256	1.0149	2.0299	3.0448
<b>32</b>	1.3438	1.3336	0.4972	0.9944	1.4916
<b>64</b>	1.3594	1.3423	0.4002	0.8004	1.2006
<b>128</b>	1.3516	1.3493	0.3483	0.6966	1.0449
<b>256</b>	1.2789	1.3574	0.3323	0.6645	0.9968
<b>512</b>	1.3125	1.3587	0.3290	0.6580	0.9871
<b>1024</b>	1.3085	1.3604	0.3282	0.6563	0.9845

stabilizing around 1.36 ppm for large filter sizes. This suggests that the moving average filter not only reduces variability but also yields a more stable estimate of the underlying clock skew. Furthermore, while the median is zero for small  $N$  (up to  $N = 8$ ), it aligns closely with the mean for larger  $N$ , indicating a more symmetric and less skewed distribution of the filtered estimates as the averaging window increases.

Overall, these results confirm that employing a larger moving average window leads to more reliable clock skew estimates. Hence, the maximum filter size is used for offset prediction.

### B. Offset Measurements

A screenshot of the oscilloscope displaying the two rectangular signals that are used for evaluation on Channel 1 (C1) and Channel 4 (C4) is shown in Figure 6, with the trigger level set to half of the maximum signal voltage. In this screenshot, the measurement cursors indicate that the temporal offset between the two signals is approximately 4.8 ns. To derive statistical probabilities, a series of 500 measurements was carried out

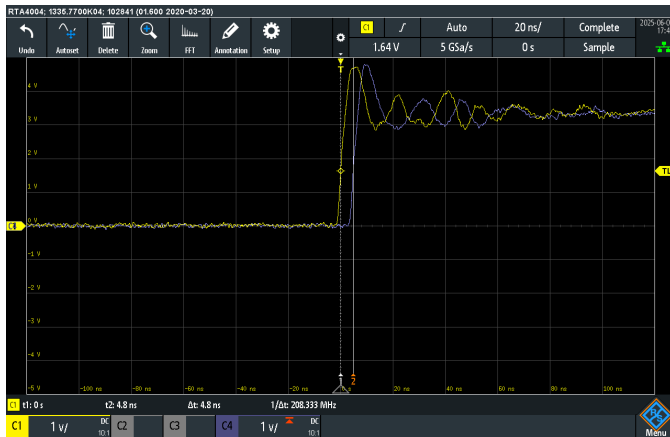
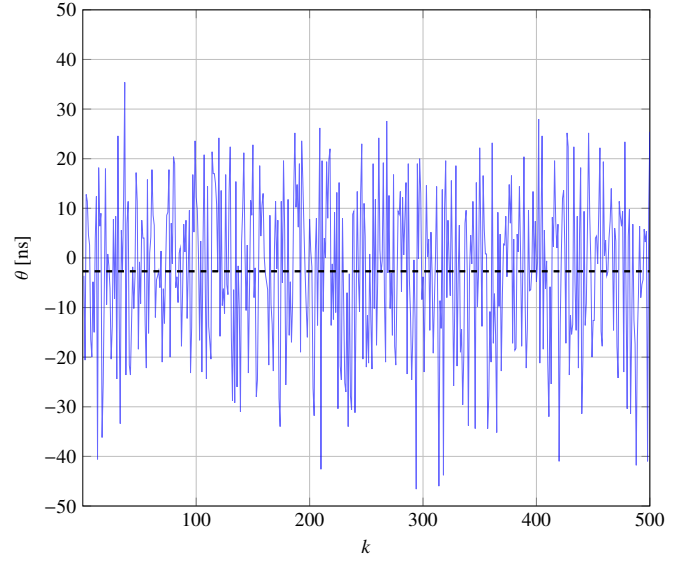
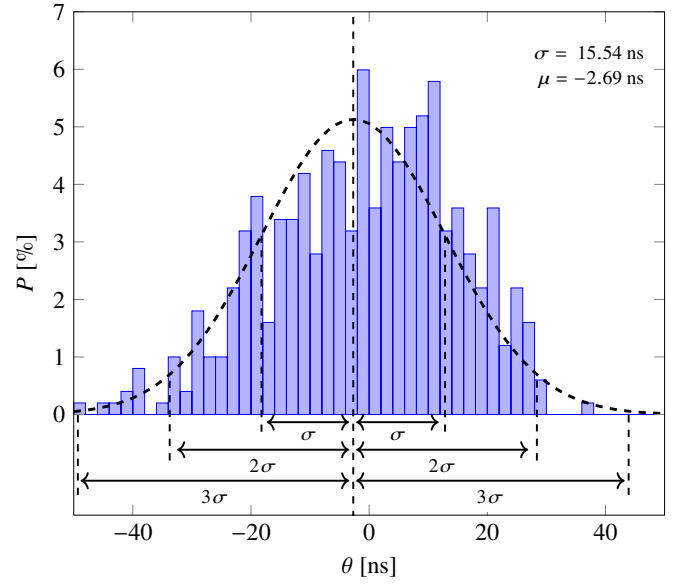


Figure 6. Oscilloscope screenshot showing the two rectangular validation signals captured on two channels, the trigger, and the measurement cursors.

and analyzed. The number of measurements was limited to 500 because a preliminary analysis showed that increasing the sample size beyond this point did not significantly improve the statistical power or reduce variance further. Collecting more data would have required disproportionately higher experimental effort and processing time without providing additional insights. The results are depicted in Figure 7, whereas Figure 7a shows the time series and Figure 7b both histogram and probability density function of the offset that has been measured by the oscilloscope. Additionally, Table III presents the precision in terms



(a) Time series obtained for the readings of  $\theta$ .



(b) Histogram of the probability density function obtained for the readings of  $\theta$ .

Figure 7. Results of the measurements of the offset between the two rectangular signals.

of the measured clock offset its associated standard deviations. The mean clock offset is approximately 2.69 ns, indicating a

Table III  
MEASURED CLOCK PRECISION FOR DIFFERENT STANDARD DEVIATIONS.

	$\sigma$	$2\sigma$	$3\sigma$
$E(\theta = \mu)$ [ns]	$-2.69 \pm 15.54$	$-2.69 \pm 31.07$	$-2.69 \pm 46.61$
$P[\%]$	68.27	95.45	99.73

slight systematic bias, while the spread of the measurements increases with higher standard deviation intervals. Specifically, for  $1\sigma$  the offset is within  $\pm 15.54$  ns with a probability  $P = 68.27\%$ . For  $2\sigma$ , the interval widens to  $\pm 31.07$  ns with a probability of 95.45 %, and for  $3\sigma$ , the maximum observed spread is  $\pm 46.61$  ns with a probability of 99.73 %. These results confirm that the proposed synchronization scheme achieves high precision, with the vast majority of offset estimates confined to a narrow interval of less than 50 ns even under very conservative confidence levels. The small mean offset further indicates minimal systematic error in the clock alignment.

## VII. CONCLUSION

This paper tackled the challenge of achieving sub-microsecond time synchronization in wireless systems, focusing on industrial applications and 5G networks. We proposed and enhanced a robust protocol capable of synchronizing UEs, gNB, and 5GC, making it suitable for hybrid network deployments. The solution was implemented on a hardware testbed using OAI and SDRs, with performance evaluated through moving average filters of varying sizes. Results showed that a filter size of 1024 yields the highest precision by effectively reducing high-frequency noise and stabilizing clock skew estimates.

Experimental validation in a controlled laboratory environment demonstrated synchronization precision within  $\pm 50$  ns, which is an order of magnitude better than the one microsecond target, highlighting the approach's feasibility for high-precision industrial 5G and 6G networks. While real-world factors such as propagation delay may introduce additional challenges, adding TA information can compensate for these effects. Overall, the achieved precision provides a strong margin to meet the stringent timing requirements of time-sensitive industrial applications, confirming the effectiveness of the proposed synchronization method for practical deployment.

## REFERENCES

- [1] E. Gibney, "What time is it on the Moon?" *Nature*, vol. 614, no. 7946, pp. 13–14, 2023. DOI: 10.1038/d41586-023-00185-z.
- [2] M. Wollschlaeger, T. Sauter, and J. Jasperneite, "The Future of Industrial Communication: Automation Networks in the Era of the Internet of Things and Industry 4.0," *IEEE Industrial Electronics Magazine*, vol. 11, no. 1, pp. 17–27, Mar. 2017. DOI: 10.1109/MIE.2017.2649104.
- [3] D. Chandramouli, P. Andres-Maldonado, and T. Kolding, "Evolution of Timing Services From 5G-A Toward 6G," *IEEE Access*, vol. 11, pp. 35 150–35 157, 2023. DOI: 10.1109/ACCESS.2023.3265213.
- [4] M. Lipiński, T. Włostowski, J. Serrano, and P. Alvarez, "White Rabbit: a PTP Application for Robust Sub-nanosecond Synchronization," in *2011 IEEE International Symposium on Precision Clock Synchronization for Measurement, Control and Communication*, 2011, pp. 25–30. DOI: 10.1109/ISPCS.2011.6070148.
- [5] P. Chen and Z. Yang, "Understanding Precision Time Protocol in Today's Wi-Fi Networks: A Measurement Study," in *2021 USENIX Annual Technical Conference (USENIX ATC 21)*, 2021, pp. 597–610.
- [6] A. Morato, E. Ferrari, C. Zunino, *et al.*, "IEEE 1588 (PTP) Over mmWave 5G NR: Preliminary Assessment of the Synchronization Accuracy for TSN Applications," in *2024 IEEE 29th International Conference on Emerging Technologies and Factory Automation (ETFA)*, 2024, pp. 1–4. DOI: 10.1109/ETFA61755.2024.10710776.
- [7] G. Cena, S. Scanzio, A. Valenzano, and C. Zunino, "Implementation and Evaluation of the Reference Broadcast Infrastructure Synchronization Protocol," *IEEE Transactions on Industrial Informatics*, vol. 11, no. 3, pp. 801–811, 2015. DOI: 10.1109/TII.2015.2396003.
- [8] M. Gundall, J. Schneider, H. D. Schotten, *et al.*, "5G as Enabler for Industrie 4.0 Use Cases: Challenges and Concepts," in *2018 IEEE 23rd International Conference on Emerging Technologies and Factory Automation (ETFA)*, vol. 1, Sep. 2018, pp. 1401–1408. DOI: 10.1109/ETFA.2018.8502649.
- [9] A. Mahmood, M. I. Ashraf, M. Gidlund, *et al.*, "Time Synchronization in 5G Wireless Edge: Requirements and Solutions for Critical-MTC," *IEEE Communications Magazine*, vol. 57, no. 12, pp. 45–51, 2019. DOI: 10.1109/MCOM.001.1900379.
- [10] I. Godor, M. Luvisotto, S. Ruffini, *et al.*, "ALook Inside 5G Standards to Support Time Synchronization for Smart Manufacturing," *IEEE Communications Standards Magazine*, vol. 4, no. 3, pp. 14–21, 2020. DOI: 10.1109/MCOMSTD.001.2000010.
- [11] P. Rost, D. Chandramouli, and T. Kolding, "5G plug-and-produce: How the 3GPP 5G System facilitates Industrial Ethernet deployments to fuel Industry 4.0 applications," Apr. 2020. [Online]. Available: <https://onestore.nokia.com/asset/207281>.
- [12] M. K. Atiq, R. Muzaffar, O. Seijo, *et al.*, "When IEEE 802.11 and 5G Meet Time-Sensitive Networking," *IEEE Open Journal of the Industrial Electronics Society*, vol. 3, pp. 14–36, 2022. DOI: 10.1109/OJIES.2021.3135524.
- [13] P. Kehl, J. Ansari, M. H. Jafari, *et al.*, "Prototype of 5G Integrated with TSN for Edge-Controlled Mobile Robotics," *Electronics*, vol. 11, no. 11, p. 1666, 2022. DOI: 10.3390/electronics11111666.
- [14] T. Striffler and H. D. Schotten, "The 5G Transparent Clock: Synchronization Errors in Integrated 5G-TSN Industrial Networks," in *2021 IEEE 19th International Conference on Industrial Informatics (INDIN)*, 2021, pp. 1–6. DOI: 10.1109/INDIN45523.2021.9557468.
- [15] M. Gundall, C. Huber, P. Rost, *et al.*, "Integration of 5G with TSN as Prerequisite for a Highly Flexible Future Industrial Automation: Time Synchronization based on IEEE 802.1AS," in *2020 46th Annual Conference of the IEEE Industrial Electronics Society (IECON)*, IEEE, vol. 1, 2020, pp. 3823–3830. DOI: 10.1109/IECON43393.2020.9254296.
- [16] M. Gundall, J. Stegmann, C. Huber, *et al.*, "Implementation and Evaluation of the RBIS Protocol in 5G," in *2022 IEEE Globecom Workshops (GC Wkshps)*, 2022, pp. 323–328. DOI: 10.1109/GCWkshps56602.2022.10008489.
- [17] M. Mongelli and S. Scanzio, "Approximating Optimal Estimation of Time Offset Synchronization With Temperature Variations," *IEEE Transactions on Instrumentation and Measurement*, vol. 63, no. 12, pp. 2872–2881, 2014. DOI: 10.1109/TIM.2014.2320400.
- [18] M. Gundall, C. Huber, and H. D. Schotten, "Extended Reference Broadcast Infrastructure Synchronization Protocol in 5G and Beyond," in *2023 IEEE 21st International Conference on Industrial Informatics (INDIN)*, 2023, pp. 1–6. DOI: 10.1109/INDIN51400.2023.10217973.